

Positron lifetime and 2D-ACAR studies of divacancies in Si

M. Hasegawa^{1,*}, A. Kawasuso¹, T. Chiba², T. Akahane², M. Suezawa¹, S. Yamaguchi¹, K. Sumino¹

¹Institute for Materials Research, Tohoku University, Sendai 980-77, Japan
(Fax: + 81-22/215-2061)

²National Institute for Research in Inorganic Materials, Namiki 1-1, Tsukuba-shi, Ibaraki 305, Japan

Received: 29 August 1994/Accepted: 25 January 1995

Abstract. We have measured positron lifetime and Two Dimensional Angular Correlation of Annihilation Radiation (2D-ACAR) distributions of Floating-Zone grown (FZ) Si specimens containing divacancies (V_2) with the definite charge states, V_2^0 , V_2^{-1} or V_2^{-2} from room temperature to about 10 K. These charge states are accomplished by an appropriate combination of dopant species, their concentration and irradiation doses of 15 MeV electrons with reference to the currently accepted ionization level of divacancies. The positron lifetime of the negatively charged divacancy increases with temperature, while that of the neutral divacancy shows little change with temperature. The positron trapping rate, obtained from lifetime and 2D-ACAR measurements, increases markedly with decreasing temperature. This is found not only for the negative divacancies but also for the neutral divacancy. We need a model which explains this temperature dependence. The 2D-ACAR distribution from positrons trapped at divacancies shows nearly the same distribution for the different charge states, which differs considerably from the case of As vacancies in GaAs studied by Ambigapathy et al. We have observed a small but definite anisotropy in the distribution of trapped positrons in V_2^- using a specimen containing oriented divacancies.

PACS: 78.70; 61.70; 61.80

The silicon divacancy V_2 is one of the main defects induced by irradiation with electrons, neutrons or ions. It is stable at room temperature, and does not recover at annealing temperatures below 200 °C. Because of its fundamental character as a vacancy-type defect in covalent

semiconductors and also its importance in technological applications, the divacancy has been studied theoretically and experimentally by many workers. Positron annihilation studies have been also done by several groups [1-8]. From these positron annihilation studies interesting physical properties have been reported. Firstly the positron trapping rate for divacancies increases markedly with decreasing temperature. It is widely known, however, that in metals positron trapping rates for vacancies or voids do not depend on temperature or decrease with temperature [9]. The temperature dependence of the trapping at the divacancy in Si is quite in contrast to the case of metals. We call this marked increase in the trapping rate with decreasing temperature the “negative temperature dependence” of positron trapping. This has been explained by a phonon-cascade model [1] or weakly bound Rydberg state model [4] for negatively charged defects. It is noted that the negative temperature dependence for divacancies has been reported by Brandt and Cheng [10] and Shimotomai et al. [11] where their divacancies could be supposed to be neutral if we consider the doping level in their specimens and the electron-irradiation conditions. Then it is very necessary to have detailed measurements of the temperature dependence for specimens with the well-defined charge states of divacancies.

Secondly the recent development of the two-dimensional angular correlation of annihilation radiation (2D-ACAR) technique provides us with detailed momentum distribution of the electron-positron pairs in the divacancies and consequently enables us to get useful information about the microscopic and electronic structure of the divacancies, as shown very recently by Ambigapathy et al. for the vacancies in GaAs [12].

In the present study the temperature dependence of positron trapping at divacancies is obtained for specimens containing well-defined charge states of neutral (V_2^0), single-minus (V_2^{-1}) or double-minus (V_2^{-2}) using positron lifetime and 2D-ACAR measurements. Further detailed anisotropy in the 2D-ACAR distribution is studied for these divacancies.

Paper presented at the 132nd WE-Heraeus-Seminar on “Positron Studies of Semiconductor Defects”, Halle, Germany, 29 August to 2 September 1994

*To whom all correspondence should be addressed

1 Experimental

The crystals in this study were grown by the floating zone method. Divacancies were introduced by 15 MeV electron irradiation at room temperature. To obtain the different charge states for divacancies, *n*- and *p*-type crystals with appropriate content of dopants were irradiated up to $8 \times 10^{17} \text{e/cm}^2$. After irradiation, the Fermi level positions were evaluated from Hall coefficient measurements by the van der Pauw method [13]. Fermi level positions are plotted against the electron dose in Fig. 1 together with the ionization levels for the divacancy. The specimens employed in this study and their characteristics are listed in Table 1. The specimens doped with P were annealed after irradiation to remove V-P pairs [7]. For the annealed specimens Hall coefficients were re-measured to obtain the Fermi level. Thus the definite charge state of the divacancy was attained by an appropriate combination of dopant species, their contents, electron-irradiation doses and post-irradiation heat treatments, as listed in Table 1. Furthermore, in order to obtain the anisotropy of the 2D-ACAR distribution for the divacancy, the specimen with the alignment of the vacancy axis direction in the lattice was employed. This was achieved by stress alignment at elevated temperature: the crystal was compressed along a [011] axis to 500 kg/cm^2 at 170°C for 1 h, then cooled to room temperature with stress on [15]. The degree of alignment, $n_{\text{in}}/n_{\text{out}}$, is estimated to be about 1.5, where n_{in} and n_{out} are the populations of the divacancies in the (011) plane and out of the plane, respectively.

Positron lifetime measurements were carried out using a conventional apparatus with time resolution of about 240 ps (FWHM). The lifetime spectra were analyzed with the PATFIT-88 program [16]. The 2D ACAR spectra were obtained with the 2D-machine of Anger camera type

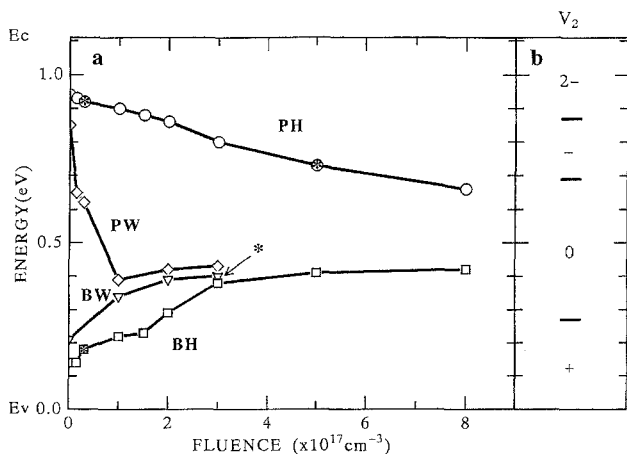


Fig. 1a,b. Shifts in Fermi level position after 15 MeV electron irradiation [6] (a) and ionization levels of divacancy in Si [12] (b). E_c shows the bottom of the conduction band, while E_v is the top of the valence band. Dopants and the levels are shown by the symbols: PH (highly doped with phosphor, P: $1.7 \times 10^{16} \text{ cm}^{-3}$); PW (weakly doped with phosphor, P: $7.0 \times 10^{14} \text{ cm}^{-3}$); BW (weakly doped with boron, B: $4.0 \times 10^{14} \text{ cm}^{-3}$); and BH (highly doped with boron, B: $1.0 \times 10^{16} \text{ cm}^{-3}$). The asterisks denote the specimens in the as-irradiated states. The Fermi levels for the specimens A and B after annealing are presented in Table 1

at the National Institute for Research in Inorganic Materials.

2 Results and discussion

2.1 Lifetime measurements

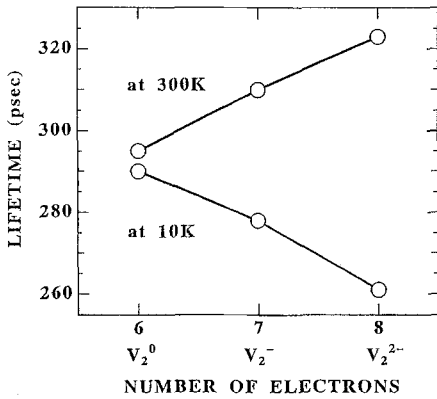
The lifetime spectra for the specimen containing divacancies of the neutral and negative charge states were well decomposed into two lifetime components with the time constants τ_i ($i = 1, 2$) and the relative intensities I_i ($I_1 + I_2 = 1$). The τ_2 component is due to positrons trapped at the divacancies. For the specimen D with positive divacancies, no second lifetime component was observed, which suggests that the positive divacancies do not trap positrons.

The lifetime τ_2 for V_2^0 shows little change with decreasing temperature from 300 K to 10 K. However, the lifetimes for the negative vacancies, V_2^{-1} and V_2^{-2} , decrease with temperature as shown in Fig. 2. It is noted that the lifetime at 10 K decreases with the number of electrons in the divacancies, as expected from the dependence of positron lifetimes on electron density. At 300 K, however, the positron lifetime increases with the number of electrons, which makes quite a contrast to the observation at 10 K. The fact that the lifetimes for the negative divacancies increases with temperature suggests the decrease in overlap integral between the wave functions of positron and electron. This probably reflects some relaxation effects such as pairing and breathing which were proposed for the single vacancy [17, 18].

With a conventional two-state trapping model the trapping rates for the divacancies with the neutral and negative charges were obtained. The trapping rates increase markedly with decreasing temperature, showing the negative temperature dependence, as seen in Fig. 3 in (a) a linear and (b) a logarithmic plot. The negative temperature dependence for the negative divacancy has been explained by a phonon-cascade trapping model [1] based on Lax theory and by two-stage shallow trapping model with Rydberg state of negatively charged vacancies [4]. In the phonon-cascade model the positron is attracted from the negative divacancy and the energy dissipation of the binding energy is accomplished with successive phonon emission whereby the temperature dependence is given by T^{-n} for $n = 1-4$ depending on detailed phonon-process. As seen Fig. 3(a) the temperature dependence above about 100 K is well given by this temperature dependence. Below 100 K, however, the temperature dependence deviates appreciably from the T^{-n} dependence. Puska et al. have claimed that the phonon cascade processes are very ineffective and proposed the two-stage trapping model with the shallow precursor (Rydberg state). This model successfully describes the temperature dependence for the single vacancy and vacancy-phosphor pairs [19]. In Fig. 3(b) their model is applied phenomenologically to the negative temperature dependence as shown by the solid lines with the shallow binding energy of 21, 11 and 9 meV for V_2^{-2} , V_2^{-1} and V_2^0 respectively. The shallow binding energies are of the correct order expected from the Rydberg state model. It should be noted, however, that the

Table 1. Characteristics of specimens. The Fermi levels were obtained from the Hall coefficient measured at room temperature

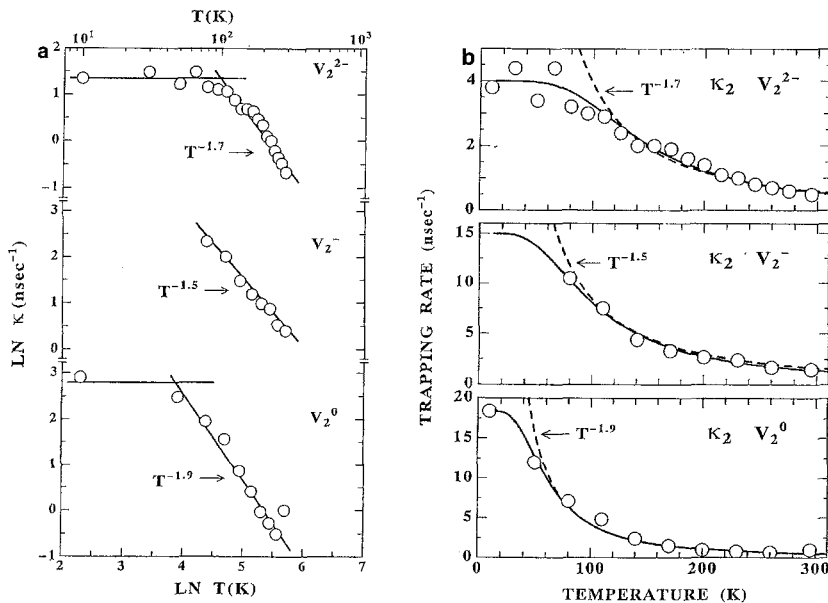
Specimen	Charge states	Dopant conc. [cm ⁻³]	Fluence [e/cm ²]	V ₂ conc. [cm ⁻³]	Fermi level* [eV]	Remarks
A	V ₂ ⁻²	P: 1.7 × 10 ¹⁶	3.0 × 10 ¹⁶	8 × 10 ¹⁴	E _c - 0.17	150°C × 0.5h annealed
B	V ₂ ⁻¹	P: 1.7 × 10 ¹⁶	5.0 × 10 ¹⁷	7 × 10 ¹⁵	E _c - 0.34	250°C × 1h annealed
C	V ₂ ⁰	B: 4.0 × 10 ¹⁴	3.0 × 10 ¹⁷	3 × 10 ¹⁶	E _v + 0.40	As irradiated
D	V ₂ ⁺¹	B: 1.0 × 10 ¹⁶	3.0 × 10 ¹⁶	7 × 10 ¹⁵	E _v + 0.17	As irradiated

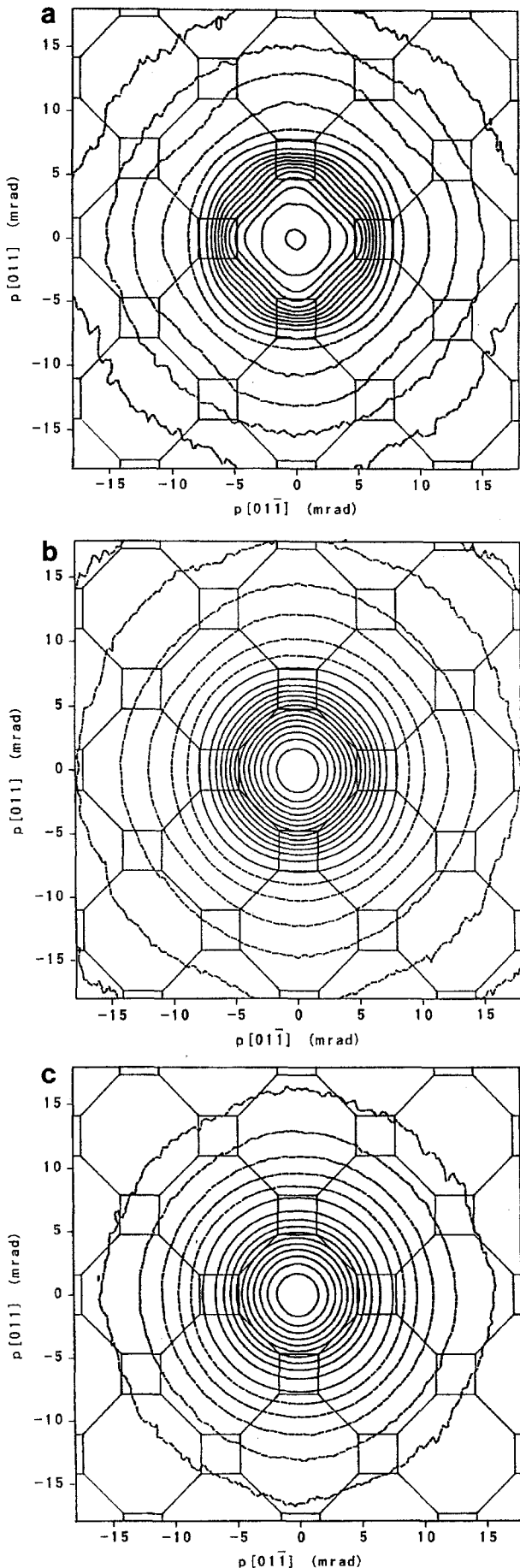
**Fig. 2.** Positron lifetime for the divacancies, V₂⁻² (specimen A), V₂⁻¹ (specimen B), and V₂⁰ (specimen C) at 10 K and 300 K.

Rydberg state model is based on the weakly bound states attained by attractive potential between positron and negative divacancy. In this sense no temperature dependence of positron trapping is expected for the neutral divacancy. Of course, the phonon cascade model also does not explain the negative temperature dependence because it also depends on Coulombic attractive potential exerted by the negative, but not neutral, divacancy.

Historically the negative temperature dependence for electron-irradiated silicon, floating-zone refined *p*-type Si, was first reported about 20 years ago by Brandt and Cheng [10]: they suggested the possibility of the shallow neutral trap of the irradiation-induced defect. Unfortunately they did not specify the irradiation-induced defects as divacancies. However according to the dose dependence of the Fermi level, their defects were considered to be the neutral divacancies. About 10 years later Shimotomai et al. [11] observed the negative temperature dependence of positron trapping, using Doppler broadening, for electron-irradiated *p*-type (B-doped) and *n*-type (undoped) silicon specimens. Considering their dopant levels and Fig. 1 the charge state for the both specimens were supposed to be neutral.

In the present study the charge state has been experimentally specified from the Fermi level position in the band gap as shown in Fig. 1 and Table 1. A possible explanation for the negative temperature dependence of the neutral divacancy may be given by a multi-phonon process with a strong coupling between the positron and the lattice around and divacancy as proposed for free carriers by deep level defects in semiconductors [20]. In the multi-phonon process model, multi-phonon emission is assumed to take place simultaneously rather than sequentially. To clarify this, detailed experimental work is now in progress.

**Fig. 3a,b.** Temperature dependence of positron trapping rate for the divacancies, V₂⁰, V₂⁻¹ and V₂²⁻: (a) logarithmic plot, and (b) linear plot. Solid and dashed lines in (b) show fitting curves for two-stage shallow trapping model and a phonon-cascade model (T⁻ⁿ), respectively



2.2 2D-ACAR measurements

Typical 2D-ACAR distributions are shown for on (100) plane in Fig. 4 for (a) unirradiated and (b) the irradiated specimen containing oriented divacancies (V_2^{-1}) (the specimen B). The 2D-ACAR distribution of the unirradiated specimens shows large anisotropies due to the fact that the $3p$ -orbitals on the two sites in a unit cell of Si tend to have opposite phases in order to form covalent bonding [21]. However the 2D-ACAR distribution of the specimen with the oriented divacancies shows only a small anisotropy, which suggests very isotropic 2D-ACAR distribution.

The 2D-ACAR distribution can be decomposed into a centrally symmetric isotropic part and an anisotropy. We have found for the all the specimens (A, B and C) we measured that the anisotropies do not change their shapes within the experimental error, but only differ in their amplitudes. Therefore, we can assume that almost all the anisotropies come from the positrons annihilating in the bulk (perfect lattice) of the specimens. Thus we take the ratio of the amplitude (valley to peak altitude) of the anisotropy of a specimen to that of the unirradiated specimen as a measure of the bulk annihilation component in the specimen. Our previous study [8] revealed that, with reference to the anisotropies of the unirradiated specimen, we can get the bulk annihilation component of each specimen at each temperature so as to reproduce the amplitude of the anisotropy. Subtracting this bulk component gives the remaining distribution which comes from the trapped component from the divacancies. This trapping component is found to be centrally symmetric for each measurement. The trapped component intensity, for example about 73% in Fig. 4b, has been found to agree quite well with that from lifetime experiments. The 2D-ACAR distribution of the trapped component for the specimen containing the oriented divacancies are shown in Fig. 4c. We see a more isotropic distribution for the trapping component and a more isotropic distribution for the trapped component than that shown in Fig. 4b.

The small but apparent anisotropy of the trapped 2D-ACAR component is expected to provide us with useful information about electronic and microscopic structure in the divacancy. The anisotropy may be smeared by averaging with respect to four possible divacancy orientations (four equivalent $[111]$ -type orientations). Then to get the definite anisotropic distribution, we measured the distribution for the oriented divacancies. As stated above, by the stressing method the preferred orientation of the divacancy were achieved: the population of the "in-the (011)-plane" divacancies (n_{in}) is 50% higher than that of the "out-(011)-plane" (n_{out}). This inequivalence has been found in the anisotropy for the

Fig. 4a-c. 2D-ACAR distribution on (100) plane: (a) unirradiated specimen, (b) the specimen containing oriented divacancies V_2^{-1} , and (c) the trapped component for oriented V_2^{-1} . The trapped component intensity is about 73%. The solid lines stand for contours of 8.7% step of the peak height of the unirradiated specimen. The dashed lines denote the last step (the tail part) of the ACAR distribution in a successive way of geometrical progression with a factor of $1/2$ ($\Delta_{i+1}/\Delta_i = 1/2$)

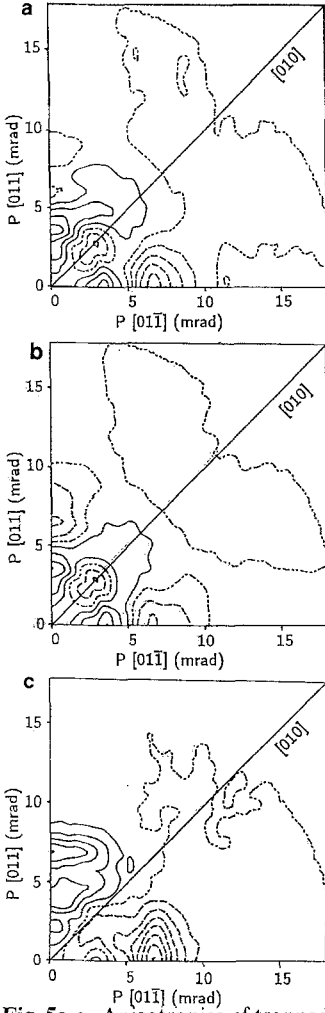


Fig. 5a-c. Anisotropies of trapped 2D-ACAR components obtained by folding as described in the text: (a) anisotropy after [011] and [011] foldings, (b) anisotropy after [011], [011] and [010] foldings, (c) Anisotropy for N_{in} (see text). Contour spacing is 0.15% of the trapped 2D-ACAR peak [8]. The *solid lines* stand for positive, the *dashed lines* for negative and the *chain lines* for the zero contour height of the anisotropy distribution

[100] 2D-ACAR distribution [8]. Then [011] and [011] directions are not equivalent. We denote the anisotropy from the divacancies lying in the (011) plane by N_{in} and that from the divacancies off the (011) plane by N_{out} . We can obtain N_{in} as follows. The anisotropy after [011] and [011] foldings, shown in Fig. 5(a), corresponds to $1.2N_{in} + 0.8N_{out} = 0.4N_{in} + 0.8(N_{in} + N_{out})$, as expected from $n_{in}/n_{out} = 1.5$. We further folded the anisotropy of Fig. 5(a) along [010] and obtained Fig. 5b, which corresponds to $(N_{in} + N_{out})$. Then we subtracted 2 times of the anisotropy in Fig. 5b from 2.5 times of that in Fig. 5a to get the anisotropy for N_{in} shown in Fig. 5c. This anisotropy has a peak around 7 mrad in the [0 1 1] direction and an accompanying valley around 7 mrad in the [0 1 1] direction as seen in Fig. 5c, considerably differing from that found in the unirradiated specimen. In the anisotropy of the 2D-ACAR distribution of the unirradiated specimen, peaks have been seen around 5 mrad in the [0 1 1] and [0 1 1] directions and valley around 5 mrad in the

[0 1 0]-direction [8]. Furthermore, the amplitudes of the anisotropies relative to the 2D-ACAR peak height are very small: 1.4% for (a), 0.9% for (b), and 1.8% for (c) of Fig. 5. As stated above, these anisotropies are quite small when compared to the anisotropy (16.9%) of the 2D-ACAR (100) distribution for the unirradiated specimen. These observations reflect the electronic structure and the relaxation effects around the divacancy. Then we expect that the anisotropy shown in Fig. 5c has indispensable information about the electronic and microscopic structure of the divacancy, and encourages further study including theoretical calculations.

We have obtained the anisotropies for unoriented V_2^0 , V_2^{-1} and V_2^{-2} divacancies which barely exceed the experimental uncertainties and correspond to Fig. 5b for these specimens: the anisotropy amplitude relative to the trapped 2D-ACAR peaks are 1.0% for V_2^0 , 0.8% for V_2^{-1} and 0.8% for V_2^{-2} .

Quite recently Ambigapathy et al. [12] have successfully applied the 2D-ACAR measurements to the study of native vacancies in GaAs and have shown marked difference in trapped 2D-ACAR distributions between a neutral (V_{As}^0) and negative (V_{As}^{-1}) vacancy. In the present study, however, only a small difference in the 2D-ACAR distribution for trapped components was observed among V_2^0 , V_2^{-1} and V_2^{-2} . Then a first-principle calculation, as done for the vacancy V_{As}^{-1} by Gilgien et al. [22], is very necessary to clarify the physical origin of this small difference.

3 Summary

We prepared specimens containing divacancies with definite charge state, V_2^0 , V_2^{-1} and V_2^{-2} by adoption of appropriate dopant species, dopant levels and electron-irradiation doses. On these specimens, positron lifetime and two-dimensional angular correlation of annihilation radiation (2D-ACAR) measurements were carried out at temperatures from 10 to 300 K. The positron lifetime for the negative divacancies increases with temperature, while that for the neutral divacancy exhibits little change on cooling down to 10 K. At 10 K the positron lifetime decreases with number of electrons in the vacancy as expected simply from the electron density at the divacancy. On the other hand, at room temperature the lifetime increases with the number of electrons, which suggests relaxation effects around the divacancies at higher temperature. The positron trapping rates at the divacancies increase remarkably with decreasing temperature. This strong temperature dependence is observed not only for the negative divacancy but also the neutral one. The 2D-ACAR distribution from the divacancy show very small change with the charge state and temperature. The anisotropy of 2D-ACAR distribution is found to be very small, less than 1% for the peak height of the 2D-ACAR distribution. We have observed the anisotropies for the oriented divacancy V_2^{-1} using a specimen containing oriented divacancies. These experimental results await theoretical calculations to clarify the positron and electron states in the divacancies in Si.

Acknowledgements. We thank Dr. K. Masumoto and the technical staff of the Laboratory of Nuclear Science, Tohoku University for their help in electron irradiation.

References

1. S. Dannefaer, G.W. Dean, D.P. Kerr, B.G. Hogg: Phys. Rev. B **14**, 2709 (1976)
2. P. Mascher, S. Dannefaer, D. Kerr: Phys. Rev. B **40**, 1764 (1989)
3. M.J. Puska, C. Corbel: Phys. Rev. B **38**, 9874 (1988)
4. M.J. Puska, C. Corbel, R.M. Nieminen: Phys. Rev. B **41**, 9980 (1990)
5. Y.K. Cho, H. Kondo, T. Kubota, H. Nakashima, T. Kawano, A. Uedono, T. Kurihara, S. Tanigawa: Mater. Sci. Forum. **105-110**, 925 (1992)
6. A. Kawasuso, M. Hasegawa, M. Suezawa, S. Yamaguchi, K. Sumino: Hyperfine Interact **84**, 397 (1994)
7. A. Kawasuso, M. Hasegawa, M. Suezawa, S. Yamaguchi, K. Sumino: Mater. Sci. Forum (submitted)
8. T. Chiba, A. Kawasuso, M. Hasegawa, M. Suezawa, T. Akahane, K. Sumino: Mater. Sci. Forum (submitted)
9. For example, K. Petersen: In *Positron Solid State Physics*, ed. by W. Brandt, A. Dupasquier (North-Holland, Amsterdam 1983) p.298
10. W. Brandt, L.J. Cheng: Phys. Lett. A **50**, 439 (1975)
11. M. Shimotomai, Y. Ohgino, T. Miyahara, K. Inoue, M. Doyama: In *Positron Annihilation*, ed. by P.G. Coleman, S.C. Sharma, L.M. Diana (North-Holland, Amsterdam 1982) p.679
12. R. Ambigapathy, A.A. Manuel, P. Hautojärvi, K. Saarinen, C. Corbel: Phys. Rev. B **50**, 2188 (1994)
13. For example, K. Seeger: *Semiconductor Physics*, 5th edn. (Springer, Berlin, Heidelberg 1991) p.62
14. For example, F. Bridges, G. Davies, J. Robertson, A.M. Stoneham: J.Phys. Condens. Matter **2**, 2875 (1990)
15. G.D. Watkins, J.W. Corbett: Phys. Rev. A **138**, 543 (1965)
16. P. Kirkegaard, N.J. Pedersen, M. Eldrup: PATFIT-88, Risø-M-2740 Rep. (Risø, Denmark 1989)
17. O. Sugino, A. Oshiyama: Phys. Rev. B **42**, 11869 (1990)
18. M. Saito, A. Oshiyama, S. Tanigawa: Phys. Rev. B **44**, 10601 (1991)
19. J. Makinen, P. Hautojärvi, C. Corbel: J. Phys. C **4**, 5137 (1992)
20. H. Sumi: Phys. Rev. B **27**, 2374 (1983)
21. T. Chiba, T. Akahane: In *Positron Annihilation*, ed. by L. Dorikens-Vanpraet, M. Dorikens, D. Segers (World Scientific, Singapore 1989) p.674
22. L. Gilgien, G. Galli, F. Gygi, R. Car: Phys. Rev. Lett. **72**, 3214 (1994)